American Mineralogist, Volume 95, pages 1052–1059, 2010

Integral molar absorptivities of OH in muscovite at 20 to 650 °C by in-situ high-temperature IR microspectroscopy

KAZUYO TOKIWAI AND SATORU NAKASHIMA*

Department of Earth and Space Science, Graduate School of Science, Osaka University, Machikaneyama-cho 1-1, Toyonaka, Osaka, 560-0043, Japan

ABSTRACT

The change with temperature of IR absorption bands in OH in muscovite was studied using unpolarized in-situ high-temperature infrared microspectroscopy. The molar absorption coefficient ε at 3628 cm^{-1} for OH in muscovite at room temperature (20 °C) has been determined to be 127 ± 6 L/mol·cm. Using the orientation factor $\gamma = 0.47$ for the angle between OH vector and **c*** axis (75 ± 5°), the true molar absorption coefficient ε at 3628 cm^{-1} is determined to be 270 ± 10 L/mol·cm at 20 °C. Integral molar absorptivities are also determined from 20 to 650 °C showing no weight loss. The value decreases from 7060 ± 190 L/mol·cm^2 at 20 °C to 5190 ± 270 L/mol·cm^2 at 650 °C (26% decrease). OH orientation of muscovite sample measured by polarized IR microspectroscopy at 20 °C showed that the angle between the projection of OH vector to (001) plane (the OH′ vector) and **b** axis is 30.5° at 20 °C and did not change greatly at higher temperatures until 650 °C. The tilting of OH dipoles toward the c* axis from 75° to about 43° while keeping the same angles along **b** axis would explain the observed decrease in integral molar absorptivities at higher temperatures, but further studies are needed to clarify the OH behavior at high temperatures.

Keywords: Muscovite, OH, in-situ high-temperature IR microspectroscopy, integral molar absorptivity, OH orientation

INTRODUCTION

Water in minerals and melts is an essential factor for the dynamics of Earth and planetary materials (Aines and Rossman 1984). The concentrations of OH and H_2O in hydrous minerals and melts are often determined by IR spectroscopy at room temperature from intensities of the absorption bands of water species using the molar absorptivities [e.g., for silicate melts, Stolper (1982); Dobson et al. (1989); Ihinger et al. (1994); Dixon et al. (1995); Yamashita et al. (1999); Ohlhorst et al. (2001); Okumura et al. (2003)].

Since molar absorptivity data for OH in minerals are limited for certain minerals, several empirical relationships have been proposed for evaluating linear and integral molar absorptivities for OH in minerals where experimental data are missing (Paterson 1982; Libowitzky and Rossman 1997; Libowitzky and Beran 2004). However, direct determination of linear and integral molar absorptivities for OH in various minerals is preferable.

High-temperature IR studies have also been conducted using a heating stage, diamond cell, and sapphire cell under IR microscopes (e.g., Keppler and Bagdassarov 1993; Nowak and Behrens 1995, 2001; Shen and Keppler 1995; Withers et al. 1999). The in-situ IR technique directly measures the concentrations of OH and H_2O at high temperatures, but often lacks calibration data for high-temperature molar absorptivity. Only a few studies (Yamagishi et al. 1997; Sowerby and Keppler 1999; Withers et al. 1999; Nowak and Behrens 2001; Okumura and Nakashima 2005) have evaluated high-temperature molar absorptivities of OH and H_2O in minerals and glasses. However, more data on representative hydrous minerals are needed.

Despite being a very common hydrous mineral with only a simple OH species, only one study (Scholze 1960) at room temperature and no studies at high temperatures have evaluated the molar absorptivity in muscovite. Therefore, molar absorptivities for OH in muscovite were determined in this study by unpolarized IR microspectroscopy both at room temperature (20 °C) and at high temperatures up to 650 °C. Unpolarized IR microspectroscopy was used to apply the obtained molar absorptivities to muscovite in natural rock systems with random mica orientations. Moreover, orientation of OH in muscovite from 20 to 650 °C was also studied by polarized IR microspectroscopy.

STARTING MATERIALS

Sample characterization

The starting material used in this study is muscovite-2*M*1 from Ishikawa, Fukushima, Japan. The chemical composition of the sample was analyzed with a JEOL-JXA-8800M electron microprobe using a defocused beam (10 μm in diameter), 15 kV accelerating voltage, and 12 nA beam current. The analytical results are listed in Table 1. Minor elements such as F and Li were below the detection limit of the EMPA analysis and have not been determined.

The water content of the powdered sample was determined by thermal analysis. Thermogravimetry (TG) was carried out using a SII TG/DTA 6000 instrument from 23 to 1100 °C with a heating rate of 10 °C/min (Fig. 1). The TG curve in Figure 1 shows a weight loss of about 2% up to about 200 °C, which may be attributed to adsorbed water (Guggenheim et al. 1987). The weight loss in the range from 200 to 950 °C is 4.46 ± 0.24 wt%. Thus, the water content of muscovite was determined to be 4.46

---

* E-mail: satoru@ess.sci.osaka-u.ac.jp

0003-004X/10/0007–1052$05.00/DOI: 10.2138/am.2010.3235

± 0.24 wt%, which is consistent with the total weight percent of 95.73 wt% obtained by the EPMA analysis (Table 1). Based on the chemical compositions in Table 1 and the TG derived water content, the chemical formula of this sample can be expressed as: $(K_{0.85}Na_{0.10})(Al_{1.87}Fe_{0.16}Mg_{0.02})(Si_{3.09}Al_{0.91})O_{10}(OH)_2$.

The obtained chemical and mineralogical compositions are very close to ideal compositions of muscovite (Bailey 1984).

Sample preparation

Thin flakes of the muscovite sample were separated from the aggregate with tweezers by using perfect cleavage (001) planes. These muscovite flakes were cut with a hole puncher into circular plates of about 3 mm in diameter.

The thicknesses of the samples were measured with a laser scanning confocal microscope (LSCM) (KEYENCE, Color Laser 3D Profile Microscope VK-8500 and VK-8510) (Okumura et al. 2003). The LSCM measurements were carried out at the same positions analyzed by FTIR microspectroscopy. The refractive index of muscovite (1.60: Klein and Hurlbut 1993) was used to determine the sample thickness based on the LSCM data.

EXPERIMENTAL METHODS

Unpolarized IR microspectroscopy

Infrared (IR) spectra of muscovite plates were measured at every 20 °C step between 20 and 1000 °C, using a heating stage (Linkam TS1500) under an FTIR microscope (Jasco IRT30+FTIR620: MCT detector, ceramic IR source, and KBr beam splitter) (e.g., Okumura and Nakashima 2005). The temperature of the heating stage was elevated at a rate of 10 °C/min. All the spectra with a spectral resolution of 4 cm^{-1} were obtained by accumulating 50 scans using an aperture size of 100 × 100 µm.

Unpolarized IR transmission spectra of a sapphire plate were first acquired between 20 and 1000 °C upon heating and then down to 20 °C upon cooling at every 20 °C to be used as background spectra at each temperature. A muscovite plate was put on the sapphire plate in the heating stage and unpolarized IR transmission spectra were recorded at every 20 °C between 20 and 1000 °C and then down to 20 °C. These unpolarized transmission sample spectra were divided by the respective background sapphire plate spectra at each temperature to obtain background corrected unpolarized absorption spectra of muscovite at each temperature. In a similar way, spectra at 50 °C steps were measured between 20 and 650 °C.

Polarized IR microspectroscopy

Polarized infrared (IR) spectra of muscovite plates were measured by adding a gold wire grid polarizer in the IR microscope (IRT30). IR light transmitted through a sample passes the IR polarizer placed before the MCT detector. Polarized spectra were measured by rotating the IR polarizer from 0 to 170° in 10° steps at temperatures of 20, 100, 300, 500, and 650 °C. All the spectra with a spectral resolution of 4 cm^{-1} were obtained by accumulating 50 scans using an aperture size of 100 × 100 µm.

TABLE 1. Chemical composition of the muscovite sample determined by EMPA

Oxide	wt%
SiO_2	46.43
TiO_2	0.03
Al_2O_3	35.48
Cr_2O_3	0.01
FeO	2.78
MnO	0.02
MgO	0.15
NiO	0.01
CaO	0.00
Na_2O	0.78
K_2O	10.04
Total	95.73

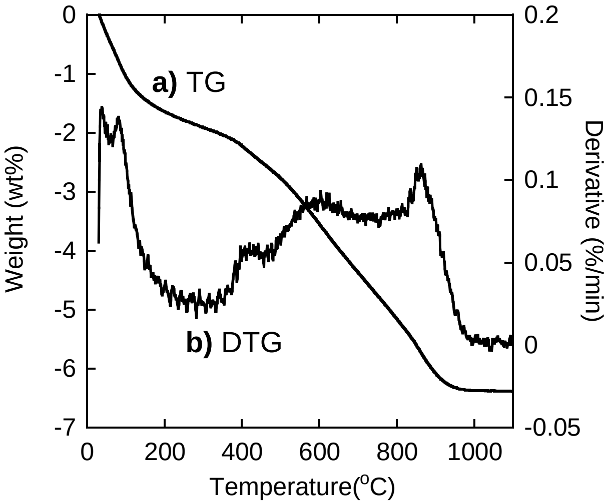

FIGURE 1. Thermogravimetry (TG) curves for the muscovite sample at a heating rate of 10 °C/min obtained by a SII TG/DTA 6000 instrument. (**a**) TG (weight loss) curve, (**b**) differential TG curve (DTG).

Polarized IR transmission spectra of a sapphire plate at 20 °C were first acquired at between 0 and 180° in 10° steps to be used as background spectra at each step. In a similar way, polarized IR transmission spectra of a sapphire plate at 100, 300, 500, and 650 °C were acquired at every 10° rotation between 0 and 180° as background spectra at each rotation and temperature step. A muscovite plate was put on the sapphire plate in the heating stage and polarized IR transmission spectra at 20 °C were recorded every 10° between 0 and 180°. Then, the sample was heated to 100 °C and polarized IR transmission spectra at 100 °C were recorded at every 10° between 0 and 180°. In a similar way, polarized IR transmission spectra at 300, 500, and 650 °C were recorded at every 10° between 0 and 180°. These polarized transmission spectra of the sample were divided by the background sapphire plate spectra at each temperature and rotational step to obtain background corrected polarized absorption spectra of muscovite.

RESULTS

Determination of molar absorptivity at 20 °C

The molar absorptivity of OH in muscovite at room temperature (20 °C) has been determined by unpolarized IR microspectroscopy. Typical unpolarized IR spectra of muscovite at room temperature (20 °C) obtained in this study are shown in Figure 2a. The absorption band around 3628 cm^{-1} is assigned to stretching vibration of OH (e.g., Gaines and Vedder 1964; Rossman 1984; Aines and Rossman 1985). The OH absorption band of muscovite appears to be consisting of three peaks at 3622, 3628, and 3650 cm^{-1}, respectively (Fig. 2a), and they will be discussed later. IR spectra of the same muscovite flakes were also measured in the simple parallel IR light in the FTIR without using the IR microscope. The obtained OH absorption band shape and intensity were identical to that obtained by using the IR microscope (Fig. 2a).

We determine the molar absorptivity ε of OH in muscovite using the Lambert-Beer law:

$$Abs = \varepsilon \cdot d \cdot C \qquad (1)$$

where *Abs* is the absorbance of OH in muscovite; ε is the molar absorptivity (L/mol·cm); *d* is the thickness of muscovite (cm); and *C* is the molar concentration of OH in muscovite (mol/L).

The peak heights at 3628 cm^{-1} (*Abs* in Eq. 1) were determined

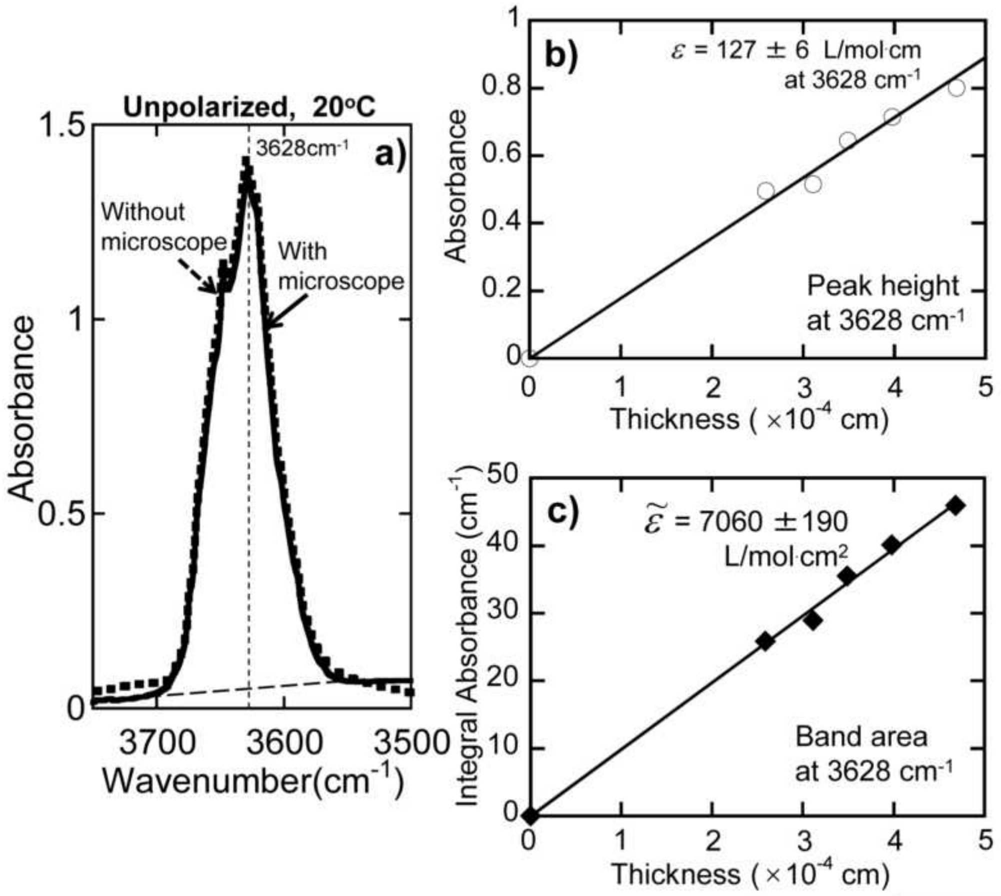

FIGURE 2. (**a**) Unpolarized IR absorption bands for OH in the muscovite flake (thickness; 7.8 μm). The spectrum measured with Cassegrainian optics under an IR microscope (solid curve) shows a band shape of OH in muscovite identical to the spectrum measured with a parallel IR beam in an FTIR without microscopic optics (dashed curve). The baseline from 3700 to 3540 cm^{-1} for determining absorbance (peak height) at 3628 cm^{-1} is also shown. (**b**) Unpolarized absorbance (peak height) at 3628 cm^{-1} as a function of the thickness of muscovite flakes. (**c**) Unpolarized integral absorbance (band area) at 3628 cm^{-1} as a function of the sample thickness.

using straight baselines in the 3700 to 3540 cm^{-1} range (Fig. 2a) for varying muscovite plate thickness. The 3628 cm^{-1} absorbance shows a linear relation with the muscovite thickness (Fig. 2b). The regression line of these data gives a gradient of 1.78 (±0.09) $\times 10^3$ (cm^{-1}) corresponding to $\varepsilon \cdot C$ in the Equation 1.

To determine the molar concentration C of OH in muscovite, thermogravimetry (TG) measurements of the powdered muscovite sample were done. Muscovite dehydration reaction involves the formation of one water molecule from two hydroxyl groups (Mazzucato et al. 1999):

$$KAl_2(Si_3Al)O_{10}(OH)_2 \rightarrow H_2O + KAl_2(Si_3Al)O_{11}. \qquad (2)$$

If the above weight loss in the range 200–950 °C of 4.46 ± 0.24 wt% (Fig. 1a) is due to water molecules lost by the reaction 2, then $M_{H_2O}/M_{mus} = 0.0446$, where M_{H_2O} and M_{mus} are the molecular weights of H_2O and muscovite, respectively. By using $M_{H_2O} = 18.02$ g/mol, M_{mus} is calculated to be 404.04 g/mol.

The molar volume of muscovite can be calculated by dividing the molecular weight of muscovite (404.04 g/mol) by its density $\rho_{mus} = 2830$ g/L (Robie et al. 1967) yielding 0.1428 L/mol. Since two moles of OH are included in one mole of muscovite, the molar concentration of OH in muscovite is obtained to be $C = 2/0.1428 = 14.0 \pm 0.75$ mol/L.

By using this molar concentration of OH ($C = 14.0 \pm 0.75$ mol/L) and the gradient $\varepsilon \cdot C = 1.78\ (\pm 0.09) \times 10^3$ (cm^{-1}) in Figure 2b, the molar absorption coefficient ε at 3628 cm^{-1} is determined to be 127 ± 6 L/mol·cm. Scholze (1960) reported this value at 3610 cm^{-1} to be 170 L/mol·cm, but without details for its determination. Our present value is smaller than this reported value (~75%), but provides the modern unpolarized determination associated with experimental details.

Paterson (1982) proposed an orientation factor γ for OH in hydrous minerals for correcting the IR absorption intensity of OH bands in unpolarized IR spectra. This factor is based on the assumption that the absorption intensity of stretching vibrations of the hydrous group is proportional to the component of the electric vector parallel to the OH dipole. If we take the orientation factor γ to be $1/2 \sin 2\alpha$, with α as the angle between OH vector and **c*** axis of 75° for ideal muscovite, the orientation factor γ becomes 0.47 in our case. By using the orientation factor $\gamma = 0.47$, the true molar absorption coefficient at 3628 cm^{-1} ε becomes 270 ± 10 L/mol·cm.

Step heating of muscovite from 20 to 1000 °C

Changes of unpolarized IR spectra of OH in muscovite as a function of temperature are shown in Figure 3a. The OH absorption band of muscovite appears to be consisting of three components at around 3622, 3628, and 3650 cm^{-1}. We have tried to simulate the OH band by two to four Gaussian components using a curve fitting program. Although the main band shape can be simulated by these Gaussian simulations, the shoulder at 3650 cm^{-1} could not be simulated. Therefore, detailed band decompositions have not been performed. Langer et al. (1981) reported OH bands for a synthetic muscovite $KAl_2(AlSi_3O_{10})(OH)_2$ located at 3629 cm^{-1} with two shoulders at 3659 and

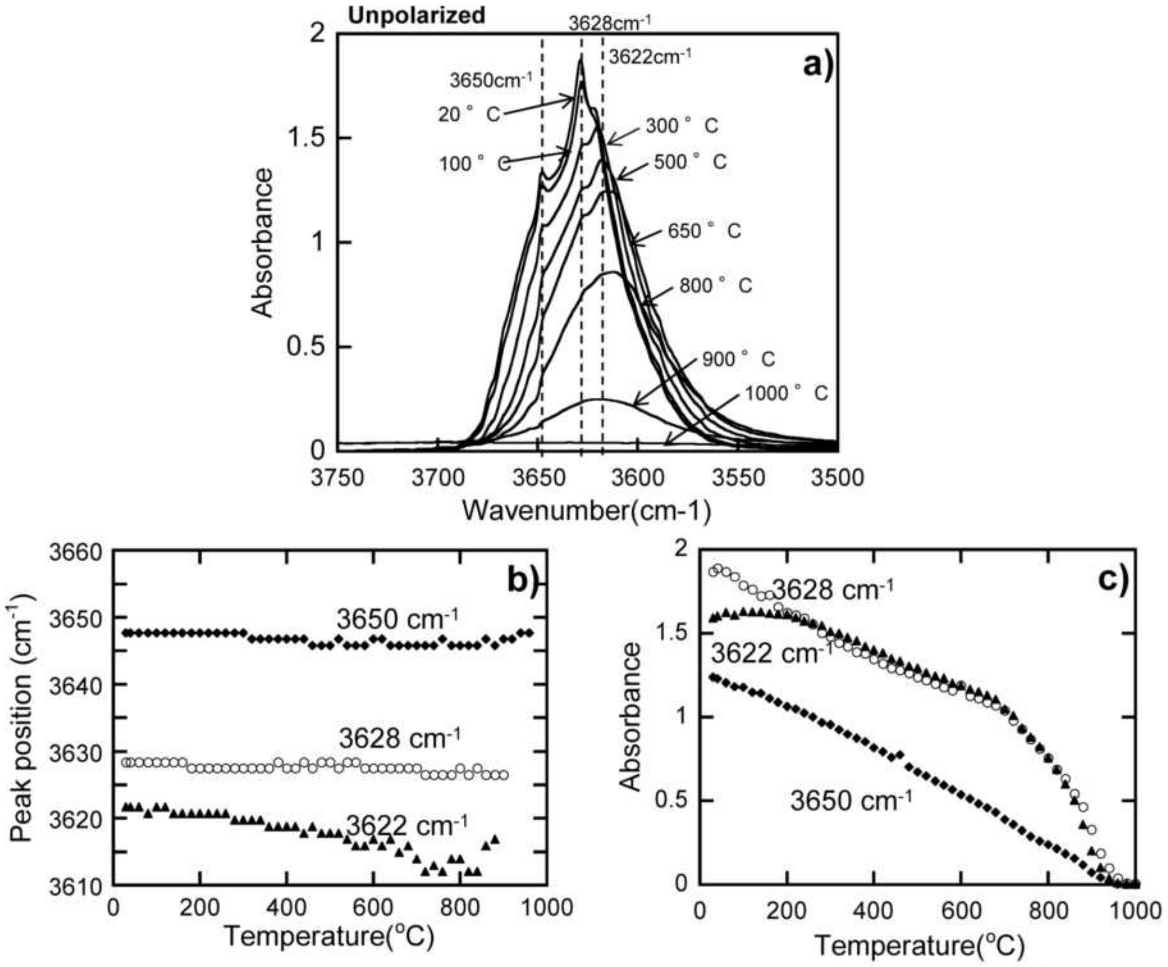

FIGURE 3. (**a**) Changes in unpolarized absorption bands around 3628 cm^{-1} due to OH in muscovite as a function of the temperature from 20 to 1000 °C. (**b**) Peak positions of 3650, 3628, and 3622 cm^{-1} peaks from 20 to 1000 °C. (**c**) Peak heights of 3650, 3628, and 3622 cm^{-1} peaks from 20 to 1000 °C.

3644 cm^{-1} together with some lower wavenumber components. They interpreted these bands to originate from different H bond interactions in various local Al/Si distributions. These bands are roughly in agreement with the 3622, 3628, and 3650 cm^{-1} bands observed in the present study.

Changes in peak positions and peak heights of the main peak at 3628 cm^{-1} and two shoulders around 3650 and 3622 cm^{-1} with temperature are presented in Figures 3b and 3c, respectively. The peak positions at 3628 and 3650 cm^{-1} showed only slight shifts within 2 cm^{-1} to the lower wavenumber up to 650 °C, while the shoulder around 3622 cm^{-1} shifted about 8 cm^{-1} to the lower wavenumber until 650 °C (Fig. 3b).

A temperature-induced peak shift of OH in mica has been reported in some studies (Gaines and Vedder 1964; Aines and Rossman 1985; Libowitzky et al. 1997; Mookherjee et al. 2001), and some of them were tentatively explained by the change in librational amplitude of hydroxyl group with temperature [Libowitzky et al. (1997) for hemimorphite; Mookherjee et al. (2001) for phengite]. Alternatively, Guggenheim et al. (1987) explained this lowering of OH band frequency by the approaching of octahedral Al toward OH resulting in the weakening of O-H bond.

The peak height at 3650 cm^{-1} decreased quasi-linearly with temperature over the entire temperature range (20 to 950 °C) (Fig. 3c). Those at 3628 and 3622 cm^{-1} showed also a similar linear trend between 200 and 650 °C. Above 650 °C a much more rapid decrease was observed. Three OH band components showed a similar behavior of peak height decrease in the 200–650 °C range, which resulted in the quasi-linear decrease in the integral molar absorptivity of OH in muscovite up to 650 °C, discussed later. The rapid decrease of peak heights at 3628 and 3622 cm^{-1} above 650 °C should be related to muscovite dehydration (Tokiwai and Nakashima 2009). The different behavior of the 3650 cm^{-1} peak above 650 °C can be due to its more independent isolated nature in the muscovite structure. The constant peak height of 3622 cm^{-1} component up to 200 °C might be originated from its strongly H-bonded nature.

Changes in the total band area around 3628 cm^{-1} from 20 to 1000 °C are shown in Figure 4a. The band areas were determined using straight baselines in the 3700 to 3540 cm^{-1} range (Fig. 2a). The band area decreased quasi-linearly from 20 to 650 °C and then rapidly approaching zero around 950 °C (Fig. 4a). The OH band around 3628 cm^{-1} could be recovered to the initial value upon cooling from 650 to 20 °C. TG of a muscovite flake sample showed no weight loss under 650 °C (Gridi-Bennadji and Blanchart 2007). Therefore, temperature-induced changes in band area of OH in muscovite under 650 °C are due to changes in its physicochemical states without dehydration. Figure 4b shows the normalized band area from 20 to 650 °C. These data are average values for four samples. The OH band area decreased to 82% of the room-temperature value at 590 °C (Fig. 4b), and this is in agreement with the 84% decrease at the same temperature reported by Aines and Rossman (1985).

Determination of integral molar absorptivities of OH in muscovite at 20–650 °C

The average values of the 3628 cm^{-1} band areas for four muscovite samples, normalized to their initial values at 20 °C show a quasi-linear decrease from 20 to 650 °C, where the decrease attained about 26% (Fig. 4b).

The integral molar absorptivity $\tilde{\varepsilon}$ can be defined as:

$$I = \tilde{\varepsilon} \cdot d \cdot C \tag{3}$$

where I is the integral absorbance (cm^{-1}); $\tilde{\varepsilon}$ is the integral molar absorptivity ($L/mol \cdot cm^2$); d is the thickness of muscovite (cm); and C is the molar concentration of OH in muscovite (mol/L).

The integral molar absorptivity $\tilde{\varepsilon}$ at 20 °C can be calculated from the band area vs. sample thickness relationship in Figure 2c. The gradient of the fitted line gives the values of $\tilde{\varepsilon} \cdot C = 9.88\ (\pm 0.26) \times 10^4\ cm^{-2}$. By using the molar concentration of OH ($C = 14.0 \pm 0.75$ mol/L), the integral molar absorption coefficient $\tilde{\varepsilon}$ of the 3628 cm^{-1} band at 20 °C is determined to be 7060 ± 190 $L/mol \cdot cm^2$.

For the determination of high-temperature integral molar absorptivities $\tilde{\varepsilon}$, the changes in d and C with temperature should be considered. The increase in the molar volume of muscovite is estimated to be less than 1% based on the expansivity data until 650 °C reported by Mazzucato et al. (1999). Therefore, the sample thickness does not change significantly at higher temperatures. The band area around 3628 cm^{-1} recovered mostly to their initial value upon cooling from 650 to 20 °C indicating no significant water loss during the high-temperature IR measurements. Thus, the thickness d and molar concentration C can be considered to be unchanged for higher temperatures.

The changes with temperature in the integral absorbance (band area) observed in Figure 4b can therefore be directly attributed to temperature-induced changes of the integral molar absorptivity $\tilde{\varepsilon}$. By applying the integral molar absorptivity $\tilde{\varepsilon}$ at 20 °C (7060 ± 190 $L/mol \cdot cm^2$) to the results in Figure 4b, the $\tilde{\varepsilon}$ value decreases from 7060 ± 190 $L/mol \cdot cm^2$ at 20 °C to 5190 ± 270 $L/mol \cdot cm^2$ at 650 °C (26% decrease). By using the orientation factor $\gamma = 0.47$, the true integral absorption coefficient is 15 020 ± 400 $L/mol \cdot cm^2$ at 20 °C.

Paterson (1982) determined this value to be 23 400 $L/mol \cdot cm^2$ at 20 °C using the data of Scholze (1960) (11 000 $L/mol \cdot cm^2$) with the orientation factor $\gamma = 0.47$. Based on the polarized IR measurements of Rouxhet et al. (1970), the value ranges from 21 000 to 23 000 $L/mol \cdot cm^2$ (Beran 2002). Therefore, the present value of the integral molar absorptivity $\tilde{\varepsilon}$ of OH in muscovite by unpolarized measurements is much smaller from the reported values (65–70%). Origins of this difference in the integral molar absorptivity from the reported values are not known.

DISCUSSION

Absorption probability

IR absorption intensity is related to absorption probability per unit time (e.g., Strickler and Berg 1962). Therefore, the observed OH band area decrease with temperature in muscovite can be originated from the decrease in the probability of the transition from the ground state to the excited state leading to IR absorption, since the population of each state will change with temperature. Boltzmann factor determines the relative probability P_i of a state i in a multi-state system in thermodynamic equilibrium at temperature T. The relative probability P_i of a state i can be defined as:

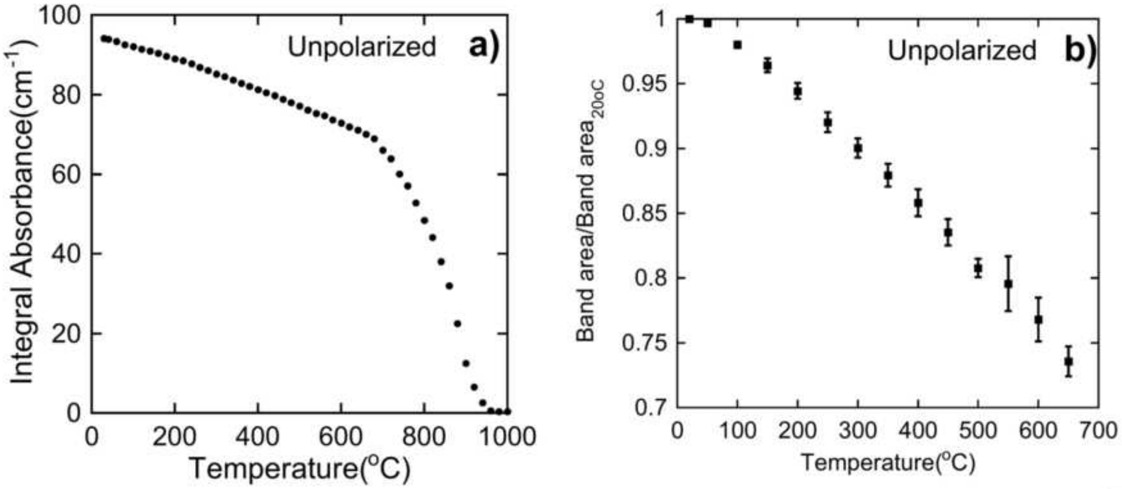

FIGURE 4. (**a**) Changes with temperature from 20 to 1000 °C in the unpolarized integral absorbance (band area) around 3628 cm^{-1} due to OH in muscovite. (**b**) The unpolarized 3628 cm^{-1} band area from 20 to 650 °C without dehydration normalized to that at 20 °C.

$$P_i \propto \exp\left(-\frac{E_i}{k_B T}\right) \tag{4}$$

where k_B is the Boltzmann constant (J/K): E_i is the energy of state i (K).

The Boltzmann factor at 3620 cm^{-1} is determined to be 2.88 × 10^{-8} and 1.18 × 10^{-3} at 20 and 650 °C, respectively. Although the probability of the excited state can increase greatly at higher temperatures, these values are both very small close to zero and not enough to explain the above decrease with temperature of the integral molar absorptivity.

The change of OH orientation

OH in muscovite at room temperature is in Al-centered octahedral layer and the position of H has been studied by IR spectroscopy (Tsuboi 1949; Serratosa and Bradley 1958; Vedder and McDonald 1963; Rothbauer 1971), neutron diffraction (Rothbauer 1971; Catti et al. 1989), and energy calculation (Abbott 1994; Liang and Hawthorne 1998). Table 2 summarizes angles between OH dipole and crystallographic axes reported in the literature (Fig. 5b). Table 2 shows that the angle between OH′ [OH′ is the projection of OH to (001) plane] and **b**-axis is about 30° and the angle between OH and **c***-axis is 75 ± 5°. However, OH orientation of muscovite at high temperatures is not known.

Therefore, we have conducted polarized infrared microspectroscopy of muscovite flakes at high temperatures. We adopted in this study a configuration that IR light emitted from FTIR spectrometer passes through an IR polarizer after transmitting a sample, which was also used by Shinoda and Aikawa (1993) and Libowitzky and Rossman (1996).

A sharp absorption peak at 3628 cm^{-1} due to stretching vibration of OH (e.g., Gaines and Vedder 1964; Rossman 1984; Aines and Rossman 1985) is observed in the polarized IR absorption spectra of muscovite at room temperature (20 °C) (Fig. 5a). Polarized IR absorption spectra were measured by changing the angle between the electric vector of IR light and the principal direction of a muscovite flake by 10° steps by rotating the IR polarizer placed before the detector. The peak heights at 3628 cm^{-1} of polarized spectra at each degree were normalized to that of the unpolarized spectra at 20 °C. The obtained peak heights (absorbances) of OH in muscovite were plotted against the angle from the **b** axis of a sample flake (Fig. 5c). The peak height shows maxima around 0 and 180° and minima around 90 and 270°.

TABLE 2. Reported angles between OH and crystallographic axes for OH in muscovite in the literature

The angle between OH′† and **b** axis	The angle between OH and **c*** axis‡	Measuring methods	Reference
–	81(?)	IR with polarized light	Tsuboi (1949)
32	74	IR with polarized light	Vedder and McDonald (1963)
–	82.8	–	Güven (1971)
30	78	Neutron diffraction	Rothbauer (1971)
–	74	IR	Rothbauer (1971)
–	78	Energy calculation	Soboleva and Mineeva (1981)
–	78	Electron diffraction	Tsipursky and Drits (1977)
–	85 ± 1	Powder neutron diffraction	Catti et al. (1994)

† OH′ is the projection of OH.
‡ **c*** axis is perpendicular to both **a** and **b** axes.

Figure 5b shows OH orientation projected on the **a-b** plane, proposed by Vedder and McDonald (1963). In this study, according to Paterson (1982), maximum (1.38) and minimum (0.48) data in Figure 5c correspond to the value of $a\cos^2\beta$ and $a\sin^2\beta$, where a is the cell constant and β (30.5°) is the angle between the OH′ vector (OH′ is the projection of OH to **a-b** plane, Fig. 5b) and **b** axis. This value is in good agreement with the reported values for β = 30° (Rothbauer 1971); 32° (Vedder and McDonald 1963) (Table 2) for muscovite.

High-temperature polarized IR absorption spectra of muscovite were measured by changing the angle between the electric vector of IR light and the principal direction of a muscovite flake (**b** axis) as explained in the experimental section. The peak heights at 3628, 3650, and 3622 cm^{-1} at higher temperatures all show a maximum around 0° and a minimum around 90° as for that at 3628 cm^{-1} at 20 °C (Fig. 5c). Changes with the polarization angle in the integral absorbance (band area) are similar showing maximum absorption around 0°–10° and a minimum around 90–100° (Fig. 5d). The integral absorbance decreased to about 73% around 0–10° and to about 77% around 90–100° at 650 °C (Fig. 5d). The angles between the OH′ vector and **b** axis can be calculated from the band area data to be 30.8° at 20 °C and 31.0° at 650 °C, respectively, and they are considered to remain unchanged for high temperatures.

OH dipoles in muscovite are considered to have angles of about 32–30° with respect to the **b** axis and 75° to the **c*** axis and Vedder and McDonald (1963) proposed that two OH dipoles are symmetrically inclined by keeping these angles (Fig. 5b). The projections of these two OH dipoles to the **a-b** plane are two OH′ vectors in Figure 5b. Based on this model, the polarization angles close to 0° to the **b** axis for OH in muscovite at 20 to 650 °C can be explained by keeping a symmetrical OH orientation along the **b** axis for these temperatures.

If the angles of OH dipoles to the **c*** axis, which was initially 75°, are also changed by tilting of OHs, their projection to the **a-b** plane would also change. For instance, the change from 75 to 43° to the **c***axis would result in the reduction of the OH′ length of about 25%. This would explain the observed 26% decrease of the integral molar absorptivity $\bar{\varepsilon}$ from 20 to 650 °C for OH in muscovite.

Mookherjee et al. (2001) reported the change with temperature in the OH orientation for phengite, which has a similar structure like muscovite, measured by in-situ neutron diffraction. The value of ω, the angle between the O-H vector and the normal to the (001) plane, decreased from about 25° at 100 °C to 7° at 650 °C, while the O-H bond length decreased from about 1.04 Å at 100 °C to 0.98 Å at 650 °C (Mookherjee et al. 2001). Both changes with temperature in the angles and bond lengths of OH would cause the increase with temperature of the integral molar absorptivity, which is opposite to our experimental observation. However, their IR results showed also the OH peak shift from 3602 to 3594 cm^{-1} (at 440 °C) indicating the OH bond length increase, in contradiction to the above neutron diffraction data (Mookherjee et al. 2001). The presence of more Mg in the phengite structure might also cause differences of OH behavior at high temperatures from those for muscovite.

Although some disagreement exists among reported data, the observed decrease with temperature in the integral molar

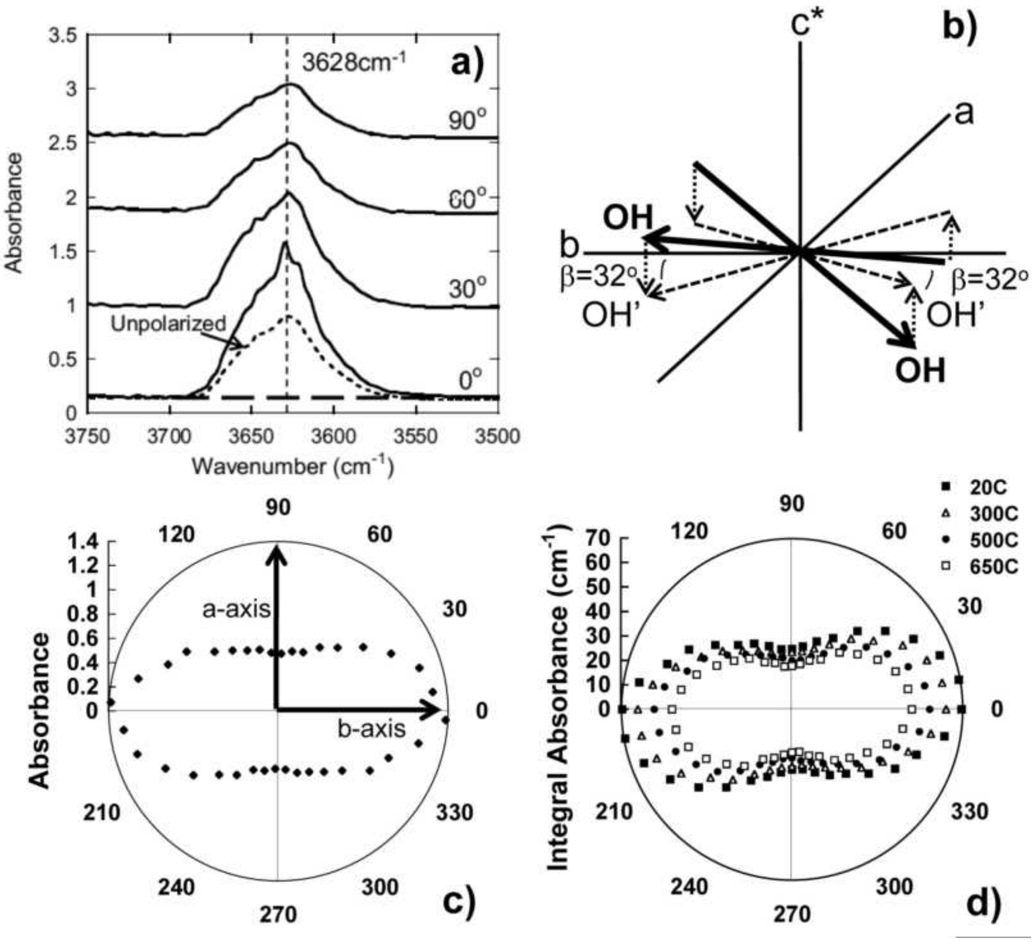

FIGURE 5. (**a**) Polarized and unpolarized IR OH bands of the muscovite sample at 20 °C. The angle of electronic vector of IR light and the principal direction of the muscovite flake (**b**-axis) was changed by the polarizer (0, 30, 60, and 90° spectra are shown). (**b**) OH directions in muscovite with respect to the crystallographic axes, proposed by Vedder and McDonald (1963). Two OHs are inclined about 75° from the **c*** axis and their projection to the **a**-**b** plane (OH′) have angles of about 32° from the **b** axis. (**c**) Changes in absorbance (peak height) at 3628 cm^{-1} with the angle of polarization at 20 °C. The absorbance is normalized to that of the unpolarized spectrum. (**d**) Changes in integral absorbance (band area) around 3628 cm^{-1} with the angle of polarization for different temperatures at 20, 100, 300, and 500 °C.

absorptivity of OH in muscovite can have a possibility of originating from the tilting of OH dipoles toward **c*** axis at higher temperatures. Further studies are needed to clarify high-temperature behavior of OH in muscovite.

ACKNOWLEDGMENTS

We are grateful to SII-NT for their kind assistance in thermogravimetry of the samples. We thank M. Yoshizaki of Tokyo Institute of Technology for her assistance of the EMPA analyses. We thank two anonymous reviewers for their thoughtful comments that greatly improved the manuscript.

REFERENCES CITED

Abbott, Jr., R.N. (1994) Energy calculations bearing on the dehydroxylation of muscovite. The Canadian Mineralogist, 32, 87–92.

Aines, R.D. and Rossman, G.R. (1984) Water in minerals? A peak in the infrared. Journal of Geophysical Research, 89, 4059–4071.

——— (1985) The high-temperature behavior of trace hydrous components in silicate minerals. American Mineralogist, 70, 1169–1179.

Bailey, S.W. (1984) Crystal chemistry of the true micas. In S.W. Bailey, Ed., Micas, 13, p. 13–60. Reviews in Mineralogy, Mineralogical Society of America, Chantilly, Virginia.

Beran, A. (2002) Infrared spectroscopy of micas. In A. Mottana, F.P. Sassi, J.B. Thompson, Jr., S. Guggenheim, Eds., Micas: Crystal chemistry and metamorphic petrology, 46, p. 351–369. Reviews in Mineralogy and Geochemistry, Mineralogical Society of America, Chantilly, Virginia.

Catti, M., Ferraris, G., and Ivaldi, G. (1989) Thermal strain analysis in the crystal-structure of muscovite at 700 °C. European Journal of Mineralogy, 1, 625–632.

Catti, M., Ferraris, G., Hull, S., and Pavese, A. (1994) Powder neutron diffraction study of 2M$_1$ muscovite at room pressure and at 2 GPa. European Journal of Mineralogy, 6, 71–178.

Dixon, J.E., Stolper, E.M., and Holloway, J.R. (1995) An experimental study of water and carbon dioxide solubilities in Mid-Ocean Ridge basaltic liquids. Part I: Calibration and solubility models. Journal of Petrology, 36, 1607–1631.

Dobson, P.F., Epstein, S., and Stolper, E.M. (1989) Hydrogen isotope fractionation between coexisting vapor and silicate glasses and melts at low pressure. Geochimica et Cosmochimica Acta, 53, 2723–2730.

Gaines, Jr., G.L. and Vedder, W. (1964) Dehydroxylation of muscovite. Nature, 201, 495.

Gridi-Bennadji, F. and Blanchart, P. (2007) Dehydroxylation kinetic and exfoliation of large muscovite flakes. Journal of Thermal Analysis and Calorimetry, 90, 747–753.

Guggenheim, S., Chang, Y-H., and Koster van Groos, A.F. (1987) Muscovite dehydration: high-temperature studies. American Mineralogist, 72, 537–550.

Güven, N. (1971) The crystal structures of 2M1 phengite and 2M1 muscovite. Zeitschrift für Kristallographie, 134, 196–212.

Ihinger, P.D., Hervig, R.L., and McMillan, P.F. (1994) Analytical methods for volatiles in glasses. In M.R. Carroll and J.R. Holloway, Eds., Volatiles in Magmas, 30, p. 67–121. Reviews in Mineralogy, Mineralogical Society of

America, Chantilly, Virginia.

Keppler, H. and Bagdassarov, N.S. (1993) High-temperature FTIR spectra of H_2O in rhyolite melt to 1300 °C. American Mineralogist, 78, 1324–1327.

Klein, C. and Hurlbut, Jr., C.S. (1993) Manual of Mineralogy after James D. Dana, 21st edition, Muscovite, p. 515–517. Wiley, New York.

Langer, K., Chatterjee, N.D., and Abraham, A. (1981) Infrared studies of some synthetic and natural 2M1 dioctahedral micas. Neues Jahrbuch für Mineralogie Abhandlungen, 142, 91–110.

Liang, J.-J. and Hawthorne, F.C. (1998) Calculated H-atom positions in micas and clay minerals. Canadian Mineralogist, 36, 1577–1585.

Libowitzky, E. and Beran, A. (2004) IR spectroscopic characterisation of hydrous species in minerals. In A. Beran and E. Libowitzky, Eds., Spectroscopic Methods in Mineralogy, 6, p. 227–279. EMU Notes in Mineralogy, Eötvös University Press, Budapest.

Libowitzky, E. and Rossman, G.R. (1996) Principles of quantitative absorbance measurements isotropic of crystals. Physics and Chemistry of Minerals, 23, 319–327.

——— (1997) An IR absorption calibration for water in minerals. American Mineralogist, 82, 1111–1115.

Libowitzky, E., Kohler, T., Armbruster, T., and Rossman, G.R. (1997) Proton disorder in dehydrated hemimorphite; IR spectroscopy and X-ray structure refinement at low and ambient temperatures. European Journal of Mineralogy, 9, 803–810.

Mazzucato, E., Artioli, G., and Gualtieri, A. (1999) High temperature dehydroxylation of muscovite-2M(1): A kinetic study by in situ XRPD. Physics and Chemistry of Minerals, 26, 375–381.

Mookherjee, M., Redfern, S.A.T., and Zhang, M. (2001) Thermal response of structure and hydroxyl ion of phengite-2M1: An in situ, neutron diffraction and FTIR study. European Journal of Mineralogy, 13, 545–556.

Nowak, M. and Behrens, H. (1995) The speciation of water in haplogranitic glasses and melts determined by in situ near-infrared spectroscopy. Geochimica et Cosmochimica Acta, 59, 3445–3450.

——— (2001) Water in rhyolitic magmas: getting a grip on a slippery problem. Earth and Planetary Science Letters, 184, 515–522.

Ohlhorst, S., Behrens, H., and Holtz, F. (2001) Compositional dependence of molar absorptivities of near-infrared OH- and H_2O bands in rhyolitic to basaltic glasses. Chemical Geology, 174, 5–20.

Okumura, S. and Nakashima, S. (2005) Molar absorptivities of OH and H_2O in rhyolitic glass at room temperature and at 400–600 °C. American Mineralogist, 90, 441–447.

Okumura, S., Nakamura, M., and Nakashima, S. (2003) Determination of molar absorptivity of IR fundamental OH-stretching vibration in rhyolitic glasses. American Mineralogist, 88, 1657–1662.

Paterson, M.S. (1982) The determination of hydroxyl by infrared absorption in quartz, silicate glasses and similar materials. Bulletin de Mineralogy, 105, 20–29.

Robie, R.A., Bethke, P.M., and Beardsley, K.M. (1967) Selected X-ray crystallographic data: molar volumes and densities of minerals and related substances. U.S. Geological Survey Bulletin, 1248, 87 p.

Rossman, G.R. (1984) Spectroscopy of micas. In S.W. Bailey, Ed, Micas, 13, p. 145–181. Reviews in Mineralogy, Mineralogical Society of America, Chantilly, Virginia.

Rothbauer, R. (1971) Untersuchung eines 2M1-Muskovits mit Neutronenstrahlen. Neues Jahrbuch für Mineralogie Monatshefte, 4, 143–154.

Rouxhet, P.G. (1970) Kinetics of dehydroxylation and of OH-OD exchange in macrocrystalline micas. American Mineralogist, 55, 841–853.

Scholze, H. (1960) Uber die quantative UR-specktroskopische Wasserbestimmung in Silikaten. Fortschritte der Mineralogie, 38, 122–123.

Serratosa, J.M. and Bradley, W.F. (1958) Determination of the orientation of OH bond axes in layer silicates by infrared absorption. The Journal of Physical Chemistry, 62, 1164–1167.

Shen, A. and Keppler, H. (1995) Infrared spectroscopy of hydrous silicate melts to 1000 °C and 10 Kbar: Direct observation of H_2O speciation in a diamond anvil cell. American Mineralogist, 80, 1335–1338.

Shinoda, K. and Aikawa, N. (1993) Polarized infrared absorbance spectra of an optically anisotropic crystal: Application to the orientation of the OH-dipole in quartz. Physics and Chemistry of Minerals, 20, 308–314.

Soboleva, S.V. and Mineeva, R.M. (1981) Stabilité de différents polytypes de micas dioctaédriques an fonctions des potentiels partiels sur les atoms. Bulletin de Minéralogie, 104, 223–228.

Sowerby, J.R. and Keppler, H. (1999) Water speciation in rhyolitic melt determined by in situ infrared spectroscopy. American Mineralogist, 84, 1843–1849.

Stolper, E.M. (1982) Water in silicate glasses: An infrared spectroscopic study. Contributions to Mineralogy and Petrology, 81, 1–17.

Strickler, S.J. and Berg, R.A. (1962) Relationship between absorption intensity and fluorescence life time of molecules. Journal of Chemical Physics, 37, 814–822.

Tokiwai, K. and Nakashima, S. (2009) Dehydration kinetics of muscovite by in situ infrared microspectroscopy. Physics and Chemistry of Minerals, 37, 91–101, DOI: 10.1007/s00269-009-0313-3.

Tsipursky, S.I. and Drits, V.A. (1977) Effectivity of the electron method of intensity measurement in structural investigation by electron diffraction. Izvestiya Akademii Nauk SSSR. Seriya Fizicheskaya, 41, 2263–2271 (in Russian).

Tsuboi, M. (1949) On the positions of the hydrogen atoms in the crystal structure of muscovite, as revealed by the infrared absorption study. Bulletin of the Chemical Society of Japan, 23, 83–88.

Vedder, W. and McDonald, R.S. (1963) Vibrations of the OH ions in muscovite. The Journal of Chemical Physics, 38, 1583–1590.

Withers, A.C., Zhang, Y., and Behrens, H. (1999) Reconciliation of experimental results on H_2O speciation in rhyolitic glass using in situ and quenching techniques. Earth and Planetary Science Letters, 173, 343–349.

Yamagishi, H., Nakashima, S., and Ito, Y. (1997) High temperature infrared spectra of hydrous microcrystalline quartz. Physics and Chemistry of Minerals, 24, 66–74.

Yamashita, S., Kitamura, T., and Kusakabe, M. (1999) Infrared spectroscopy of hydrous glasses of arc magma compositions. Geochemical Journal, 31, 169–174.

Manuscript received March 6, 2009
Manuscript accepted March 9, 2010
Manuscript handled by Pupa Gilbert